

Effects of Na₂SO₄ Concentration and Surface Shape on The Weathering of Granite During Wet-Dry Cycling

yuanpeng cao (✉ 794072428@qq.com)

Xi'an University of Science and Technology

Qiang Sun

Xi'an University of Science and Technology

Shaofei Wang

Xi'an University of Science and Technology

Zhenlong Ge

Xi'an University of Science and Technology

Zhihao Dong

Nanjing University

Qingmin Shi

Xi'an University of Science and Technology

Research Article

Keywords: Granite, salt weathering, mass loss, surface roughness, point loading hardness

Posted Date: April 30th, 2021

DOI: <https://doi.org/10.21203/rs.3.rs-392984/v1>

License: © ⓘ This work is licensed under a Creative Commons Attribution 4.0 International License. [Read Full License](#)

Version of Record: A version of this preprint was published at Environmental Earth Sciences on November 18th, 2021. See the published version at <https://doi.org/10.1007/s12665-021-10099-6>.

Abstract

The presence of salts during cyclic wet and dry conditions can cause weathering of rock and is the main cause of damage to ancient and modern buildings. Accordingly, salt weathering, especially of granite, has aroused great interest. Determining the relationship between wet-dry cycling and the physical properties of rock is of great significance to geotechnical engineering. In this paper, granite samples were processed into two shapes (round and semicircular) and subject to 0, 10, 20, 30, 40 and 50 wet-dry cycles, with the wetting achieved with 0%, 5%, 10% or 20% Na_2SO_4 solution. The mass loss, roughness and indentation hardness of granite samples all changed to some extent with cycle number, with greater changes occurring at higher salt concentrations. Rock shape also affects the extent of weathering damage, as surface area and features such as corners facilitate the ingress of salt solution.

1. Introduction

Rock weathering has long been a research focus in fields such as engineering geology and materials science. Weathering processes include physical, chemical and biological weathering. In practical engineering scenarios, rock weathering, deformation and failure usually involve water-rock interaction (Hua et al. 2017). Hadizadeh et al. (1991) pointed out that the periodic water-rock interactions caused by rainfall and evaporation and by changes in the water level of surface runoff are the main cause of change in the physical and mechanical properties of rocks, and accelerate rock weathering. Therefore, many experiments on the effects of alternating dry-wet cycles on the physicomaterial properties of rocks have been conducted. Their results show that wet-dry cycling causes varying degrees of deterioration in physical and mechanical properties such as specific gravity, apparent porosity, bulk density, elastic modulus, hardness, uniaxial compressive strength and uniaxial tensile strength (Kevin and Alida 1996; Souleymane et al. 2008; Sumner and Loubser 2008; Lin et al. 2005; Sabah and Bushra 2016; Yao et al. 2011; Zhang et al. 2014; Sun and Zhang 2018). The water-absorbing minerals that make up rock expand in the presence of water, increasing intergranular pressure. These expanding minerals cause stress absorption and release, which leads to rock fatigue (Dove and Elston 1992). Noor-e-Khuda et al. (2019) explained that water is a good solvent in rock weathering as it provides a medium in which reactions can occur; such reactions occur more rapidly in a liquid phase than in a solid phase.

Research has found that salt weathering occurs when rocks are exposed to salt solutions. During a wet-dry cycle, salt solution enters the interior of the rock through pores on the surface and fills the internal pores. A temperature rise may lead to crystallization of salt due to evaporation of water (Benavente et al. 2007). Crystals are constantly growing in rock pores and their growth is limited by the pore walls. So, if the stress on the pore walls is high enough, the rock will be damaged. Kronlund et al. (2016) pointed out that salt crystals generated in rock pores are the most damaging type of crystals to rock. Salt crystals produce different pressures depending on the size and geometry of the rock pores. Many scholars (Friedman and Gerald 1965; Olivier 2006) have calculated crystal growth pressures in single rock pores and fissures and quantitatively analysed the effect of the rock's pore-size distribution on crystal growth under dry-wet cycling. Robert et al. (2014) reported a phase transition from Na_2SO_4 in the dry state to $\text{Na}_2\text{SO}_4 \cdot 10\text{H}_2\text{O}$ in the wet state. Na_2SO_4 was dissolved during rock immersion, resulting in high supersaturation of Glauber's salt and high

crystallization pressure during the crystal growth process, which eventually led to the destruction of the material during the immersion process. Angeli et al. (2010) discussed the influences of ambient temperature and salt solution concentration on rock damage under dry-wet cycling. The results show that rock damage increases with salt solution concentration.

Granite is a traditional building material that is superior to other rock materials in terms of durability and strength. Therefore, many researchers have carried out studies on granite at various scales. Martin et al. (1998) studied the role of particle microstructure in physical and chemical weathering processes. Noor-e-Khuda et al. (2017) studied the influence of accelerated weathering under freeze-thaw cycling on the bending strength of granite. Xu et al. (2010) studied changes in the mechanical properties and microscopic pore characteristics of granite under high-temperature heat treatment. Lopez-Arce et al. (2010) studied the effect of salt crystallization on the surface roughness of granite under dry-wet cycling with Na_2SO_4 solution. However, there are few studies on the accelerated weathering of granite samples with different shapes that are exposed to salt solutions of different concentrations. Accordingly, this study used experiments to investigate the influence of sample shape (round and semicircular) on granite weathering under dry-wet cycling conditions and analysed the degree of damage caused by salt crystals precipitating from Na_2SO_4 solutions of various concentrations (0%, 5%, 10% and 20%).

2. Materials And Methods

Figure 1 shows the main experimental procedures used in this study: Samples were (a) soaked in Na_2SO_4 solution (concentration = 0%, 5%, 10% or 20%), (b) dried in an electric air-blast drying oven, (c) weighed, and (d) tested for roughness after each wet-dry cycle.

2.1 Materials

The test samples were granite with one of two shapes. As shown in Fig. 2, one shape was a 50 mm × 25 mm disk with a shear crack 18 mm long and 1.6 mm wide, and the other was a semicircular disk with a shear crack 12 mm long and 1.6 mm wide.

2.2 Wet-dry cycle testing

In this experiment, Na_2SO_4 solutions with four concentrations (0%, 5%, 10% or 20%) were prepared (Fig. 1a). Granite samples were immersed in Na_2SO_4 solution for 2 h at room temperature. After soaking, the samples were put into an electric blast-drying oven (Fig. 1b) and dried at 105 °C for 1 h. This cycle was repeated 50 times. After each cycle, samples were weighed and tested for roughness, while pressed-in hardness was measured after 50 cycles.

2.3 Mass measurement

Before starting the wet-dry cycle testing, granite samples were measured using an electronic balance with an accuracy of 0.0001 g (Fig. 1c) to obtain the initial mass m . After the start of testing, the mass m_c of the granite sample was measured after 5, 10, 15, 20, 30, 40 and 50 cycles, and the mass-loss rate was calculated using Eq. (1).

$$\Delta m = \frac{m - m_c}{m} \quad (1)$$

Where Δm is the mass loss; m is the initial mass of the granite sample (g), and m_c is the mass after a wet-dry cycle (g).

2.4 Roughness measurement

The surface roughness of granite samples was measured by a surface roughness meter (0918; Fig. 1d) with an accuracy of 0.001 mm. First, one side of each sample was polished and the initial roughness measured. Each measurement was carried out around the shear crack on the same plane to ensure that measurements were made in the same area. The surface roughness of granite samples was measured after 10, 20, 30, 40 and 50 wet-dry cycles using the four concentrations of salt solution.

2.5 Indentation hardness measurement

Indentation hardness was measured using a rock hardness tester (HYY – B; Fig. 4). Point load testing under a certain stress was carried out using a press. The experimental process is shown in Fig. 3. Load-displacement deformation curves of granite samples were obtained after 10, 20, 30, 40 and 50 cycles for each of the four Na_2SO_4 solutions (concentrations = 0%, 5%, 10% or 20%). According to the load-displacement curves, the indentation hardness and plasticity coefficient values of granite samples were calculated at each cycle number and solution concentration. Figure 3 shows the configuration of the point load ends, which provided a basis for calculating the press-in hardness.

Figure 5 shows the typical load-displacement curves of the three types of rocks. Equations (2) and (3) were used to obtain the indentation hardness and plasticity coefficient of each sample, respectively.

$$P_y = \frac{P}{S} \quad (2)$$

Where P_y is the indentation hardness (N/mm^2), P is the peak load (N) and S is the base area of the flat-bottom cylindrical indenter (mm^2). The diameter of the indenter d was 1.6 mm.

$$K_P = \frac{A_{OABC}}{A_{ODE}} \quad (3)$$

Where K_P is the plasticity coefficient, A_{OABC} is the total work expended before the rock broke (equivalent to the OABC area in Fig. 5 (b)) and A_{ODE} is the work of elastic deformation (equivalent to the ODE area in Fig. 5 (b)).

3. Results And Analysis

3.1 Macro- and micro-scale changes

Denudation of the granite samples by Na_2SO_4 solution was observed and analysed using macroscopic and microscopic images. Figures 6 and 7 show the macroscopic changes to granite samples after wet-dry cycling in the four Na_2SO_4 solutions of different concentrations. Figure 6 shows circular granite samples with signs of spalling at the edges after 50 cycles in 10% and 20% Na_2SO_4 solutions. Compared with the other three concentrations, the edge of the sample at 20% concentration showed uneven peeling. In Fig. 7, the semicircular granite sample shows slight peeling at the edges and corners after 50 cycles with 5% and 10% solutions. At the 20% concentration, there were obvious signs of spalling at 40 cycles that increased with further cycling. Because the semicircular granite sample was eroded by Na_2SO_4 solution, there were three eroded contact surfaces at the edges and corners. Therefore, peeling started from the edges and corners and then gradually spread to the centre, thereby expanding the peeling area. As a result, the overall shape of the sample became smaller and irregular, even losing the semicircular shape. When the granite sample was eroded by Na_2SO_4 solution, the rate of mineral exfoliation inside the rock was higher than that on the surface.

Figure 8 shows the microscopic changes to the granite samples. At both 5% and 10% concentrations, the edges of mineral particles were first eroded and then gradually peeled-off with increasing cycles, and only a small range of mineral particles directly peeled off. At the 20% concentration, whole dark mineral particles were directly peeled off. Under constant erosion by the Na_2SO_4 solution, the peeling area of the mineral particles gradually expanded and deepened.

3.2 Changes in mass

Table 1 shows the mass-loss rates of the granite samples. Figure 9 shows the relationship between the mass-loss rate of granite samples and number of wet-dry cycles based on the data in Table 1. While the 0% curve does not change significantly, those of the other three Na_2SO_4 solutions generally decrease first and then increase. At the beginning of a cycle, the mass-loss rate is negative, which indicates that the mass of the granite sample increases. After a certain amount of cycling damage, the mass of the sample decreases, mass-loss rate results in a positive increase. This phenomenon was more significant with the 20% Na_2SO_4 solution.

At 50 wet-dry cycles, the mass-loss rate of semicircular samples was nearly double that of circular samples. In 20% Na_2SO_4 solution, the mass-loss rate of the circular sample was 0.9907% while that of the semicircular sample was 1.7045%. The reason is that the semicircular granite samples had a greater surface area in contact with the solution than the circular samples.

Table 1 Mass-loss rates of granite samples after wet-dry cycling (%)

Na ₂ SO ₄ concentration		Cycles N _c							
		0	5	10	15	20	30	40	50
Circular samples	0%	0.0000	0.0413	0.0165	0.0247	0.0661	0.0413	0.0661	0.0909
	5%	0.0000	-0.0642	-0.0964	-0.0964	-0.0562	-0.0482	0.0241	0.0482
	10%	0.0000	-0.1490	-0.1255	-0.1412	-0.0784	-0.0156	0.0863	0.1255
	20%	0.0000	-0.2964	-0.1716	-0.0936	0.0780	0.2028	0.6630	0.9907
Semicircular samples	0%	0.0000	0.0653	0.0490	0.0653	0.0980	0.0817	0.1144	0.1307
	5%	0.0000	-0.0494	-0.0824	-0.0824	-0.0494	-0.0329	0.0329	0.0824
	10%	0.0000	-0.1136	-0.1136	-0.1299	-0.0649	-0.0324	0.0812	0.2273
	20%	0.0000	-0.2110	-0.1298	-0.0974	0.0974	0.2597	0.7792	1.7045

3.3 Changes in surface roughness

The surface roughness of granite samples is expressed by the arithmetic mean deviation (Ra). As shown in Fig. 10, in the case of the 0% Na₂SO₄ solution, the roughness did not change significantly with cycle number. In the 5%, 10% and 20% Na₂SO₄ solutions, with increasing cycles, roughness shows an increasing trend overall. This process of increase can be divided into two stages: 1) a slow stage (0–40 cycles) where roughness increases slowly with cycle number. Because the Na₂SO₄ solution left crystals on the surface of the granite or filled areas where crystals fell off, the data for each cycle fluctuated up and down slightly, with a slight increase overall. With 5%, 10% and 20% Na₂SO₄ solutions, the initial roughnesses of the circular granite samples were 0.031, 0.035 and 0.041 mm, respectively. After 40 cycles, the roughnesses of circular samples were 0.045, 0.044 and 0.050 mm, respectively, which are 0.014, 0.009 and 0.009 mm higher than their initial values. The initial roughnesses of semicircular granite samples were 0.042, 0.040 and 0.039 mm and, after 40 cycles, these increased by 0.002, 0.005 and 0.029 mm to 0.044, 0.045 and 0.068 mm, respectively. 2) The second stage is a rapid growth stage (40-50 cycles). Here, roughness increases rapidly with cycle number, most obviously with the 20% Na₂SO₄ solution. After 50 cycles with 5%, 10% and 20% Na₂SO₄ solutions, the roughnesses of circular granite samples were 0.052, 0.064 and 0.072 mm and those of semicircular granite samples were 0.054, 0.074 and 0.171 mm, respectively. Compared with that at 40 cycles, the roughnesses of circular samples were 0.007, 0.020 and 0.022 mm greater, while those of semicircular samples were 0.010, 0.029 and 0.103 mm greater.

The above results show that the concentration of Na₂SO₄ solution has a significant effect on the surface roughness of granite. The higher the concentration of salt solution, the greater the change in surface roughness.

3.4 Changes in indentation hardness

Figure 11 shows the load-displacement deformation curves derived from the point-load indentation hardness tests, which shows the deformation characteristics of the granite samples during the indentation process. The

peak load of the initial sample was the highest, with the peak values of the curves decreasing obviously with increases in the number of cycles. At a given number of cycles, the peak values decrease with increases in concentration. At 10 cycles, the peak load decreased from 4604.31 to 3382.65 as the Na_2SO_4 solution concentration increased from 0% to 20%. At 20 cycles, the peak load decreases from 4848.33 to 3658.95. At 30 cycles, the peak load decreases from 4623.56 to 3002.87. At 40 cycles, the peak load decreases from 4813.93 to 3098.40. At 50 cycles, the peak load decreases from 5122.38 to 3032.51. At a given number of cycles, the curve peak is lowest and the vertical displacement is the largest with the 20% Na_2SO_4 solution. With 0% and 5% concentrations, the deformation curves show obvious brittleness characteristics, and the relationship between load and vertical displacement is almost linear. At concentrations of 10% and 20%, the samples exhibit plastic and brittle characteristics and the curve shows a convex shape in a certain range before reaching the peak load.

Figure 12 shows the variation in indentation hardness P_y in the point-load test obtained by Eq. (2). With increasing cycle number, the fluctuation of the granite with the sample 0% solution shows almost no change, while those of samples with 5%, 10% and 20% solutions all show downward trends. The average hardness of the granite samples stays almost the same (2322.62–2333.18) between 10-50 cycles with the 0% Na_2SO_4 solution. With the 5% solution, the average hardness decreases from 2116.62 to 1839.66. At 10%, the average hardness decreases from 2041.67 to 1582.04. At 20%, the average hardness decreases from 1850.99 to 1507.38. At a given number of cycles, the greater the Na_2SO_4 concentration, the lower the indentation hardness.

Figure 13 is a graph from which the plasticity coefficient can be derived according to the initial load-displacement curves of the granite samples and Eq. (3). The plasticity coefficients were obtained by calculation, as shown in Fig. 14. It shows that at a given Na_2SO_4 concentration, the plasticity coefficient gradually increases with cycle number. The plasticity coefficient shows a linear increase with the 10% and 20% Na_2SO_4 solutions (Fig. 15). The plasticity coefficient increases from 1.41 to 1.53 over cycles 10-50 with the 5% Na_2SO_4 solution. The plasticity coefficient increases from 1.46 to 1.53 with the 10% solution and from 1.59 to 2.27 with the 20% solution. It can be seen from Fig. 16 that at a given cycle number, the higher the concentration, the lower the indentation hardness and the larger the plasticity coefficient of a granite sample. After 50 cycles, the indentation hardness and plasticity coefficient of the sample in 20% Na_2SO_4 solution were significantly different from the initial values.

4. Discussion

Initially, increases in cycle number lead to increases in sample quality, which is caused by insufficient drying (Noor-e-Khuda et al. 2017). Granite is composed of a variety of minerals that have tiny cracks between their crystals. When a granite sample is soaked, Na_2SO_4 solution enters its pores and micro-cracks. As the

temperature rises during drying, the water gradually evaporates and salt crystallization occurs. Crystals eventually form to fill the pores and cracks, making the sample more compact and with greater mass (Steiger and Asmussen 2008). At moderate cycle numbers, due to erosion by the Na_2SO_4 solution, some mineral crystals on the surface of the sample begin to fall off. The rate of mineral shedding is greater than the rate of salt crystallization inside the rock, so the mass of the sample begins to decrease. In later cycles, the mass loss changes linearly because the crystallization rate of Na_2SO_4 and the chemical reaction between the Na_2SO_4 solution and minerals in the granite stabilises. In this process, the internal pore size of the granite is constant and the salt solution constantly crystallizes in the pores, while crystal growth is restricted by the pore walls. Failure of the rock occurs when the crystal pressure exceeds the bearing limit of the pore walls, as shown in Fig. 17. As shown in Fig. 18, with increases in solution concentration, more and more minerals are shed, most of them being black minerals. Alonso et al. (2008) found that the contact between biotite and feldspar and its particles is very fragile; areas of such contact are most likely to be damaged by erosion. A large amount of biotite and feldspar shedding was also the main factor causing changes in roughness.

The experiment also found that the semicircular granite samples were degraded more than the circular ones. This indicates that the smoothness of the rock and the surface area in contact with the solution can indirectly affect the degree of weathering. At the edges and corners of rock, salt solution can penetrate into the pores from multiple directions. Crystallization pressure acts on the pore walls in different directions, causing mineral shedding to be most serious at the edges and corners.

5. Conclusions

1. The mass loss and surface roughness of granite increase with increases in wet-dry cycling. The mass loss initially decreases and then increases and accelerates with increasing numbers of cycles. The roughness changes obviously after 40 cycles. The indentation hardness of granite decreases with wet-dry cycling and becomes obviously lower after 50 cycles. The plasticity coefficient of granite increases with wet-dry cycling, with linear increases observed with 10% and 20% Na_2SO_4
2. Changes in the mass, roughness, and macroscopic and microscopic morphology of two shapes of granite samples under wet-dry cycling were analysed. Damage was more serious to semicircular samples than circular ones, indicating that the presence of edges and corroded surfaces increases the weathering effect. After 50 cycles in 20% Na_2SO_4 solution, the mass loss of the circular granite sample was 0.9907% and that of the semicircular sample was nearly double, at 1.7045%. The roughness of the circular sample increased by 0.031 mm, while that of the semicircular sample increased by 0.132 mm.
3. The effects of Na_2SO_4 solutions of different concentrations on weathering damage to granite were compared. Weathering damage increased with concentration for both shapes of samples. The higher the concentration, the more obvious the changes in mass, roughness, indentation hardness and plasticity coefficient. With increases in salt concentration, the granite properties change from brittleness to plastic brittleness.

Declarations

Acknowledgments

This research was supported by the National Natural Science Foundation of China (Grant Nos. 41972288, 41902174)

References

1. Wen Hua S, Dong F, Peng et al. Experimental investigation on the effect of wetting-drying cycles on mixed mode fracture toughness of sandstone. 2017, 93:242–249
2. Hadizadeh J, Law RD. Water-weakening of sandstone and quartzite deformed at various stress and strain rates. 1991, 28(5):431–439
3. Noor-E-Khuda, Sarkar & Albermani F (2019) FLEXURAL STRENGTH OF WEATHERED GRANITES UNDER WETTING – DRYING CYCLES: IMPLICATIONS TO STEEL STRUCTURES. *Advanced Steel Construction* 15:225–231. 10.18057/IJASC.2019.15.3.2
4. KEVIN HALL, ALIDA HALL. WEATHERING BY WETTING AND DRYING: SOME EXPERIMENTAL RESULTS. 1996, 21(4):365–376
5. Souleymane DIOP, Yujiro OGAWA, Ming ZHANG. Effects of Cyclic Wetting and Drying on Physical and Mechanical Properties of Neogene Sandstones and Siltstones from Boso Peninsula, Japan. 2008, 49(3):150–163
6. Sumner PD, Loubser MJ. Experimental sandstone weathering using different wetting and drying moisture amplitudes. 2008, 33(6):985–990
7. Lin ML, Jeng FS, Tsai LS et al. Wetting weakening of tertiary sandstones—microscopic mechanism. 2005, 48(2):265–275
8. Sabah Said Razouki, Bushra M, Salem. Frequency effect of cyclic soaking and drying on the resilient modulus of gypsum-rich roadbed sand. 2016, 7:13–20
9. Yao HY, Zhang ZH, Zhao Hui Zhu. Uniaxial Mechanical Properties of Sandstone under Cyclic of Drying and Wetting. 2011, 1269:2310–2313
10. Liang Z, Xin-Rong L, Yan F, Zi-Juan W (2014) Mechanical properties of argillaceous sandstone under wet and dry cycle in acid environment. *Electronic Journal of Geotechnical Engineering* 19:1433–1446
11. Qiang, Sun, Yuliang Zhang. Combined effects of salt, cyclic wetting and drying cycles on the physical and mechanical properties of sandstone. 2018
12. Dennis Kronlund M, Lindén, Jan-Henrik Smått. A polydimethylsiloxane coating to minimize weathering effects on granite. 2016, 124:1051–1058
13. Dove Patricia M, Elston Stephen F. Dissolution kinetics of quartz in sodium chloride solutions: Analysis of existing data and a rate model for 25°C. 1992, 56(12):4147–4156
14. Friedman G (1965) Terminology of Crystallization Textures and Fabrics in Sedimentary Rocks. *Journal of Sedimentary Research - J SEDIMENT RES* 35. 10.1306/74D7131B-2B21-11D7-8648000102C1865D
15. Olivier Coussy. Deformation and stress from in-pore drying-induced crystallization of salt. 2006, 54(8):1517–1547

16. Robert J, Flatt F, Caruso AMariaA, Sanchez et al. Chemo-mechanics of salt damage in stone. 2014, 5(1):130–135
17. Angeli M, Hébert R, Menéndez B et al. Influence of temperature and salt concentration on the salt weathering of a sedimentary stone with sodium sulphate[J]. Geological Society London Special Publications, 2010, 115(3):193–199
18. Martin R, Lee ME, Hodson I, Parsons. The role of intragranular microtextures and microstructures in chemical and mechanical weathering: direct comparisons of experimentally and naturally weathered alkali feldspars. 1998, 62(16):2771–2788
19. Noor-E-Khuda, Sarkar & Albermani F, Veidt M (2017) Flexural strength of weathered granites: Influence of freeze and thaw cycles. Construction Building Materials 156:891–901. 10.1016/j.conbuildmat.2017.09.049
20. Xu X-L, Gao F, Shen X-M, Jin C-H (2010) Research on mechanical characteristics and micropore structure of granite under high-temperature. Yantu Lixue/Rock Soil Mechanics 31:1752–1758
21. López-Arce P, Varas-Muriel MJ, Fernández-Revuelta B et al. Artificial weathering of Spanish granites subjected to salt crystallization tests: Surface roughness quantification. 2010, 83(2):170–185
22. Benavente D, Martínez-Martínez J, Cueto N et al. Salt weathering in dual-porosity building dolostones. 2007, 94(3):215–226
23. Steiger M, Asmussen S (2008) Crystallization of sodium sulfate phases in porous materials: The phase diagram $\text{Na}_2\text{SO}_4 - \text{H}_2\text{O}$ and the generation of stress[J]. Geochimica Et Cosmochimica Acta 72(17):4291–4306
24. Alonso FJ, Vázquez P, Esbert RM, et al. Ornamental granite durability: evaluation of damage caused by salt crystallization[J]. Materiales De Construccion, 2008, 58(289)

Figures

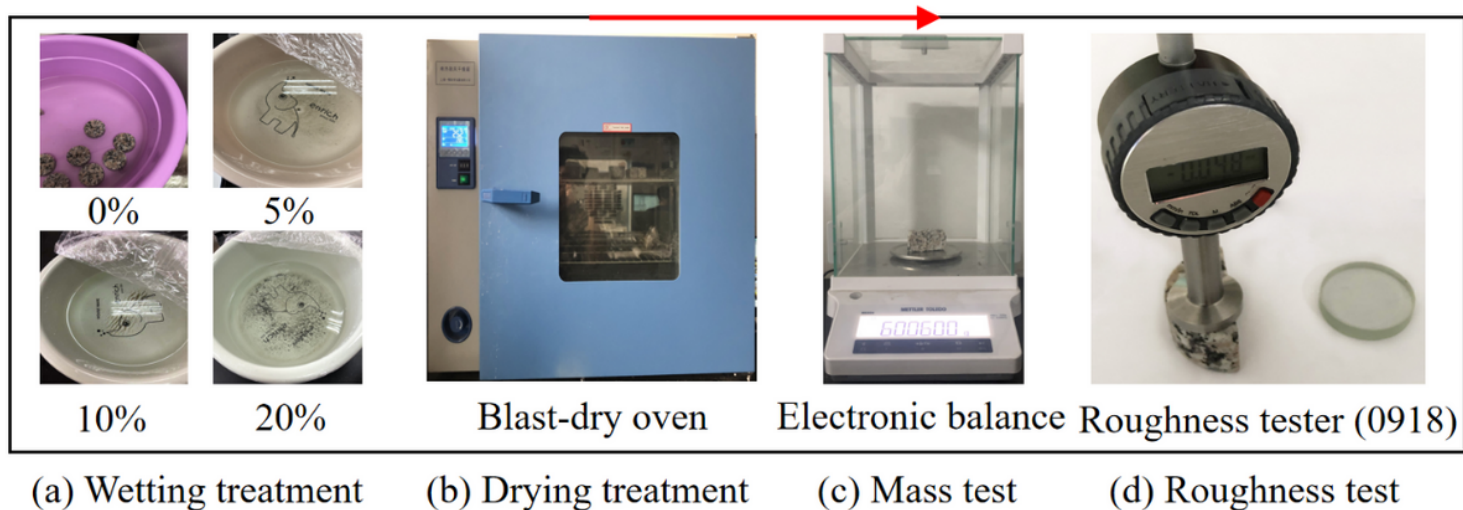


Figure 1

Test workflow

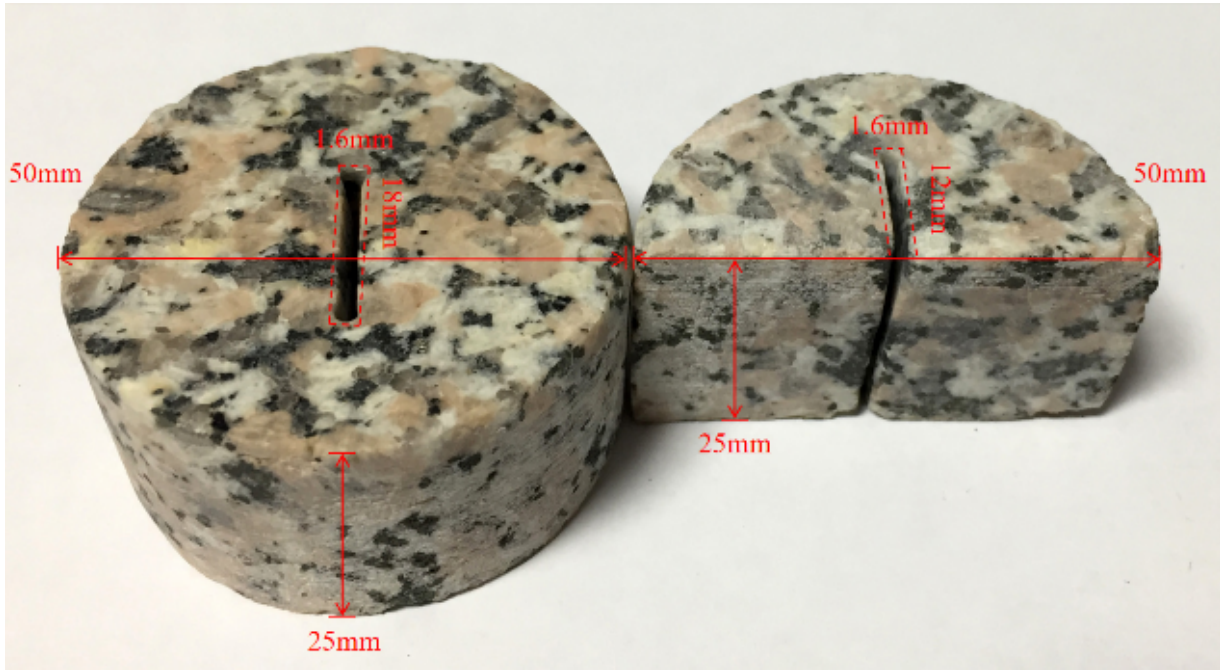


Figure 2

Photograph of granite samples

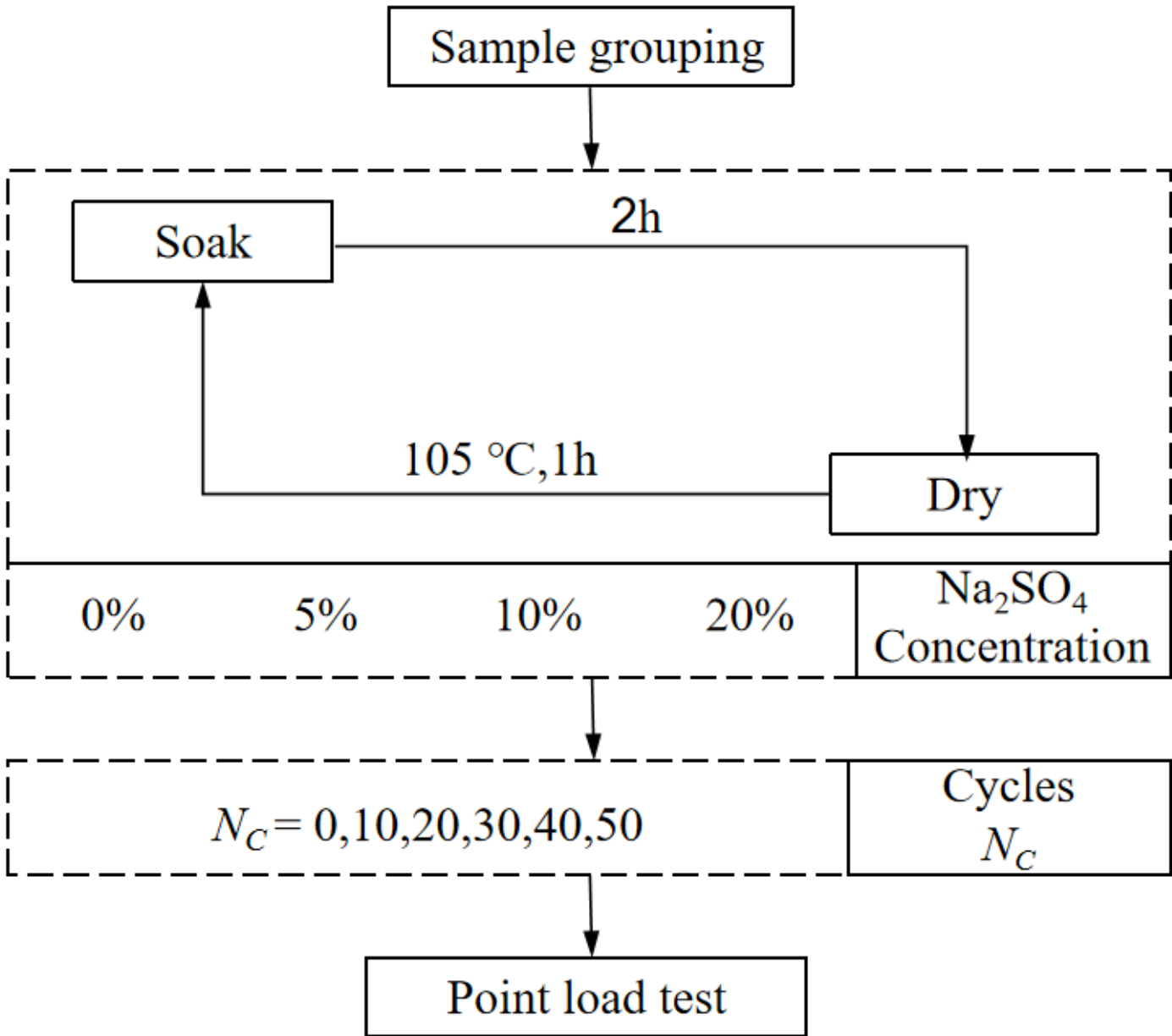


Figure 3

Point load test procedure

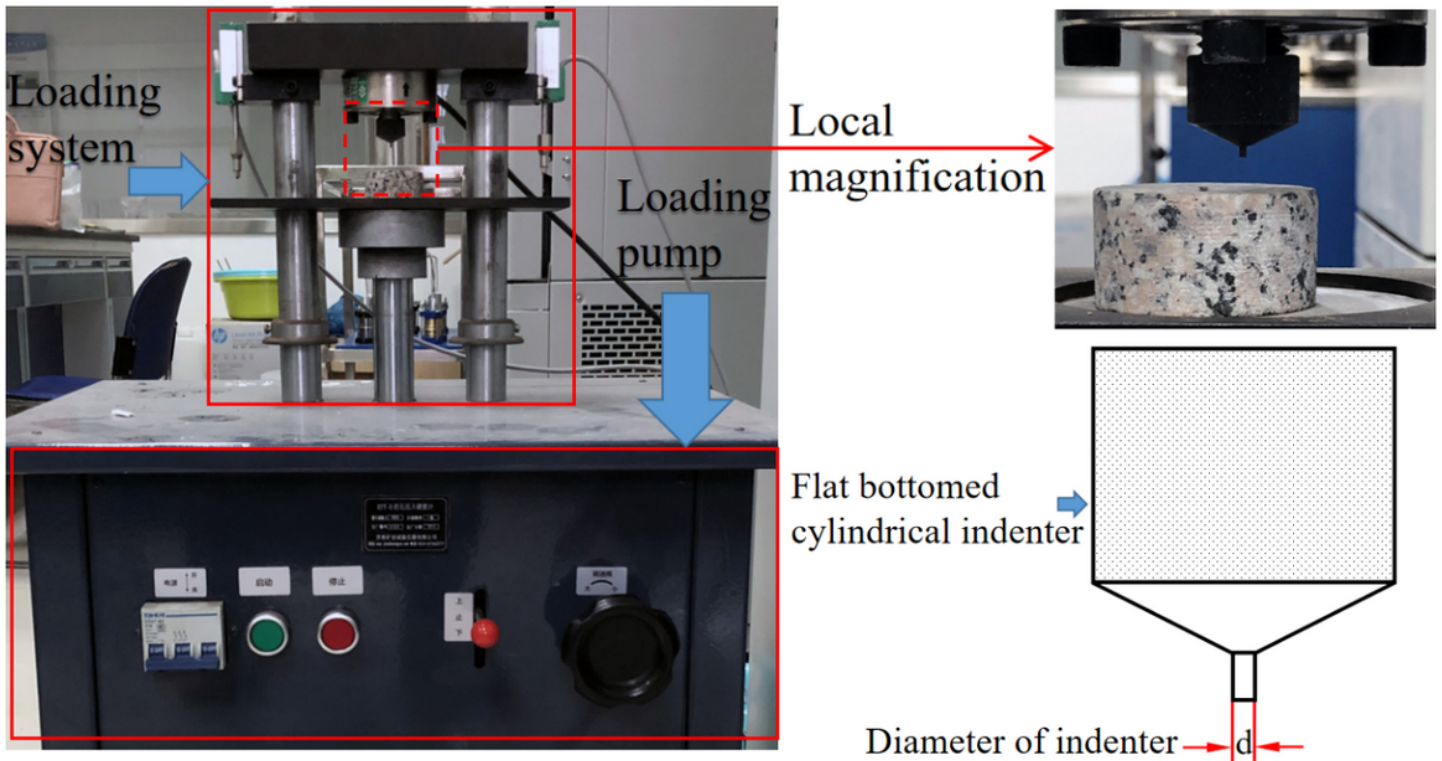


Figure 4

Photograph of the HYY-B durometer (left), close-up of rock pressing (top right) and diagram of the flat-bottom cylindrical indenter (bottom right)

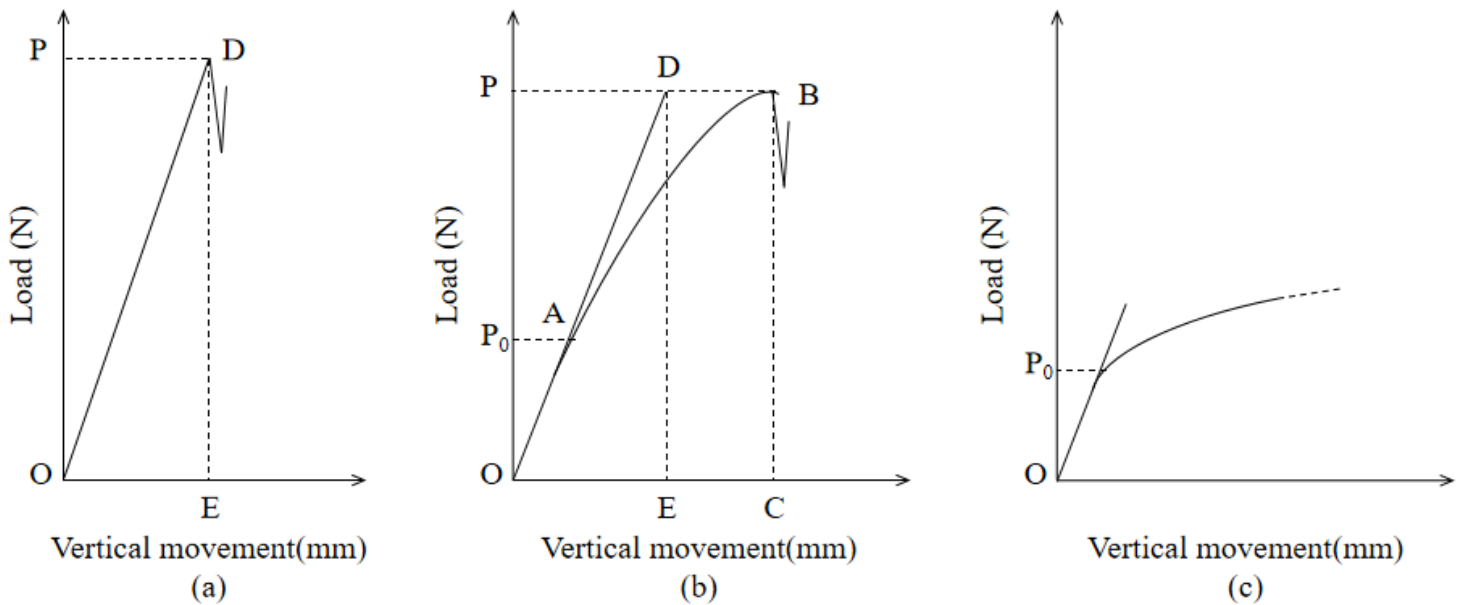


Figure 5

Load-displacement curves of flat-bottom cylindrical indenters pressed into (a) brittle rock, (b) plastic brittle rock and (c) plastic rock

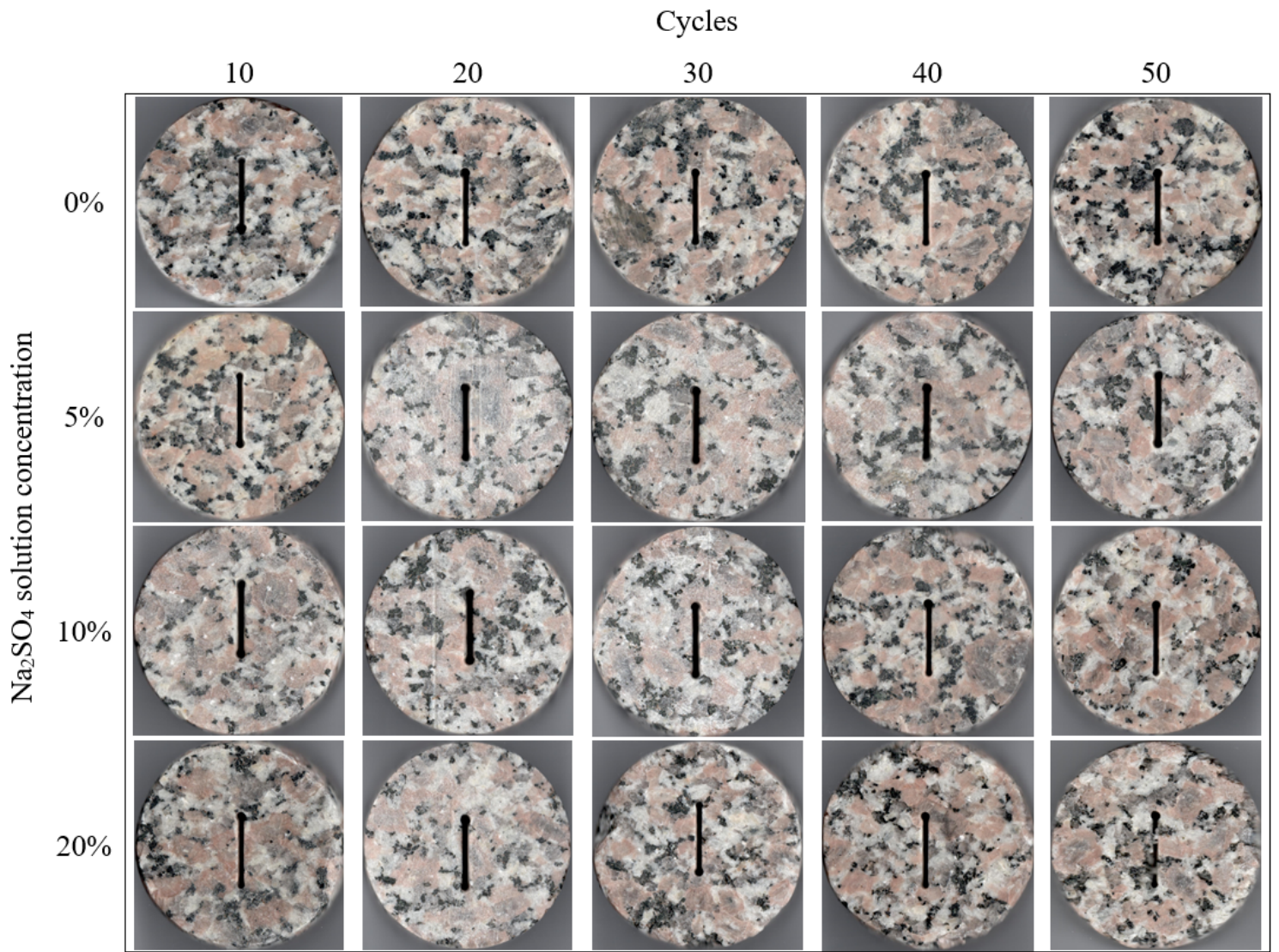


Figure 6

Comparison of macroscopic changes to round granite sample

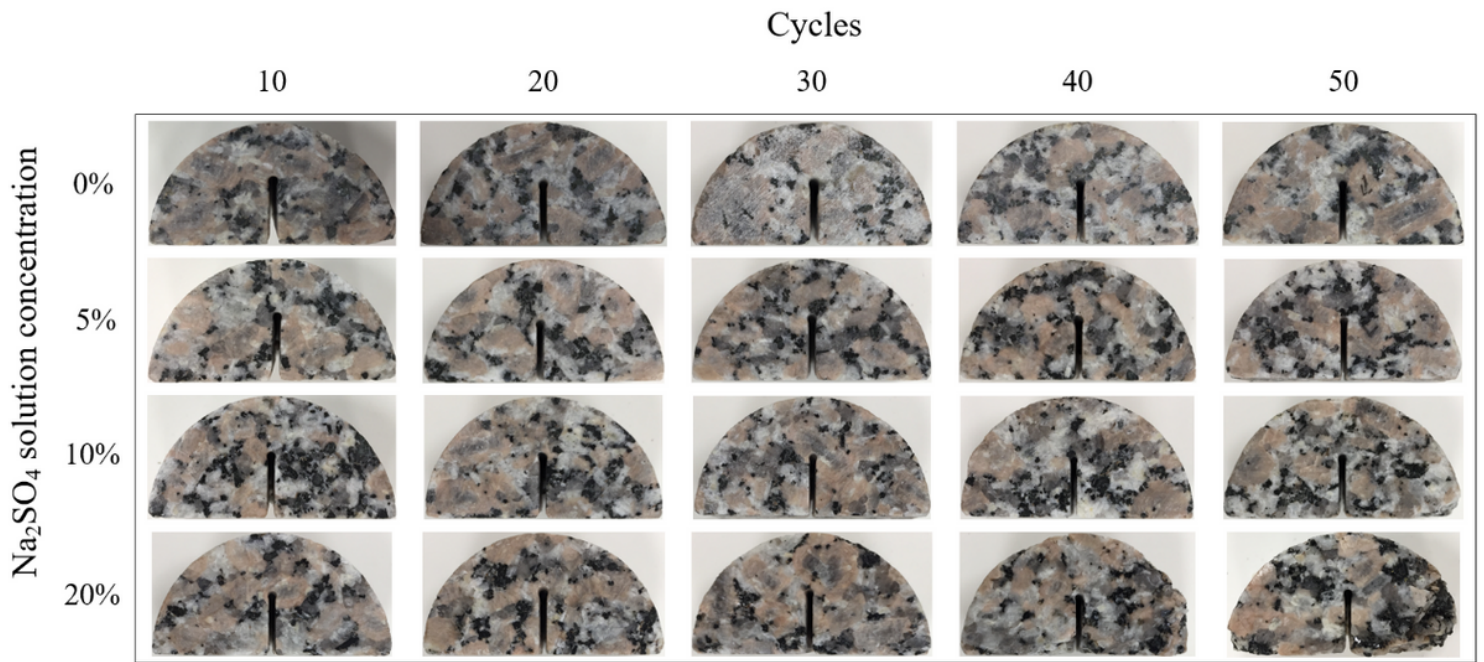


Figure 7

Comparison of macroscopic changes to semicircular granite samples

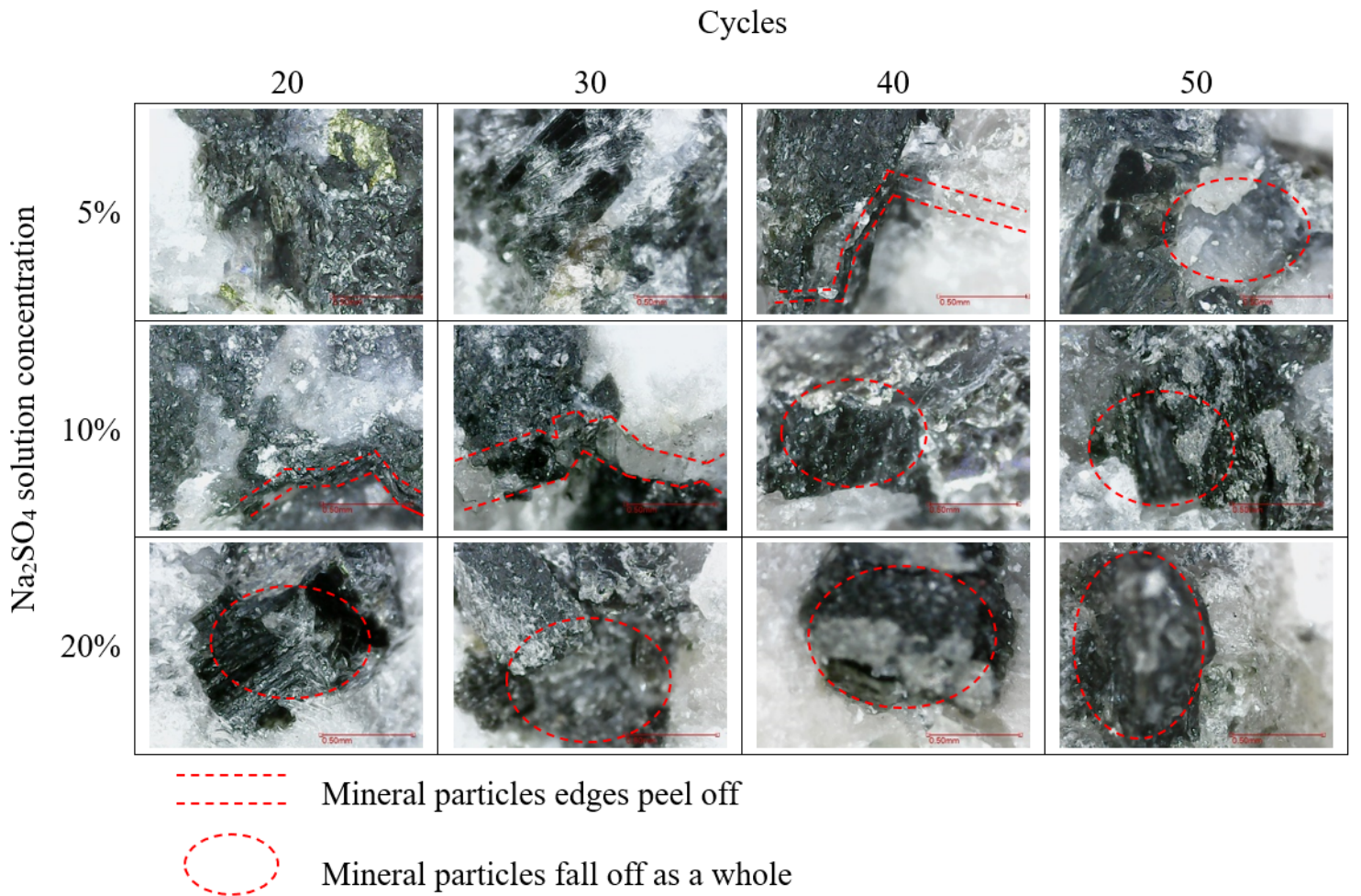


Figure 8

Comparison of microscopic changes to granite samples

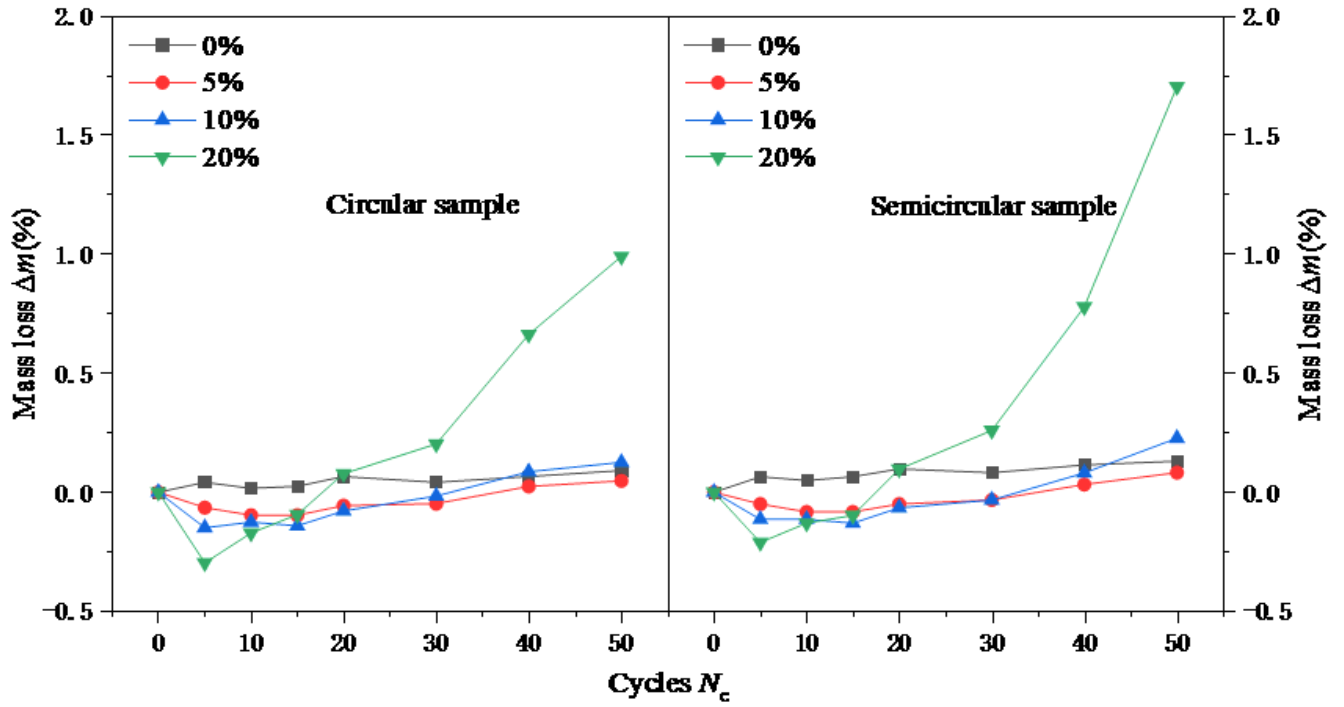


Figure 9

Relationships between the mass-loss rates of circular and semicircular specimens and cycle number

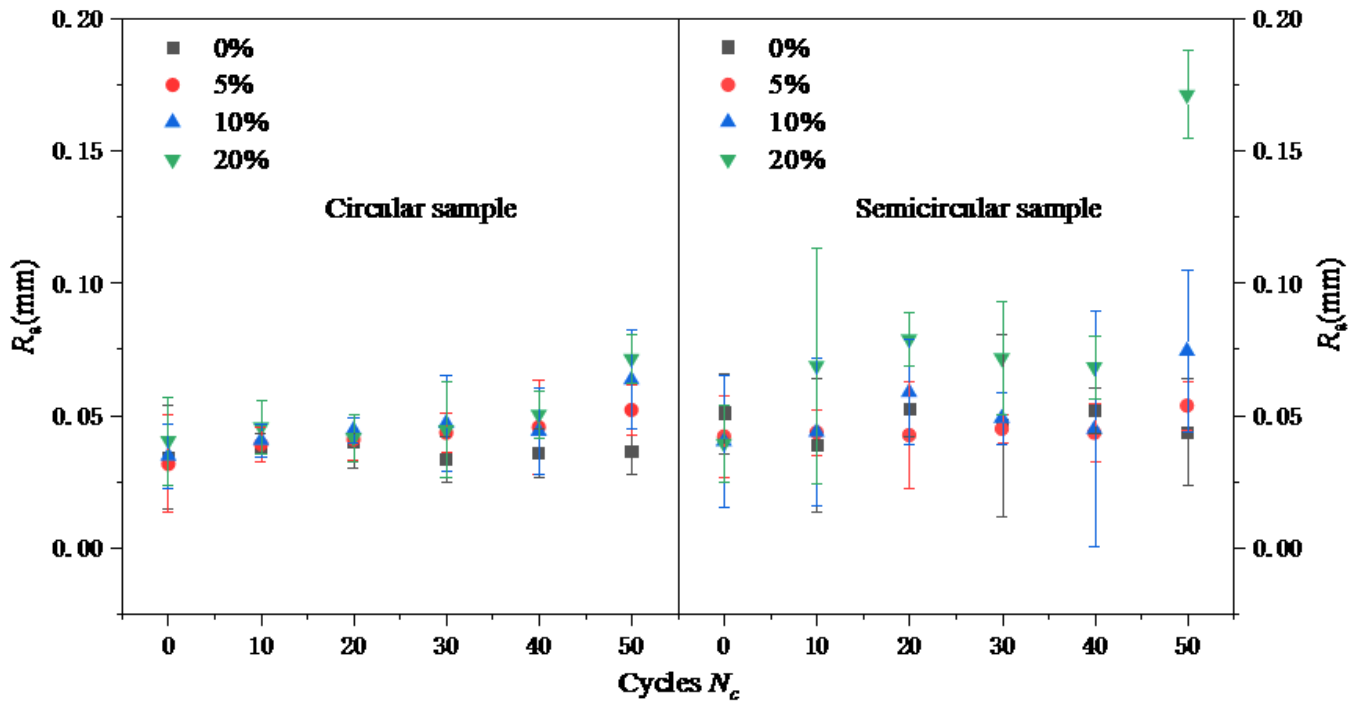


Figure 10

Relationships between wet-dry cycle number and the surface roughness of circular and semicircular granite specimens with various concentrations of Na₂SO₄ solution

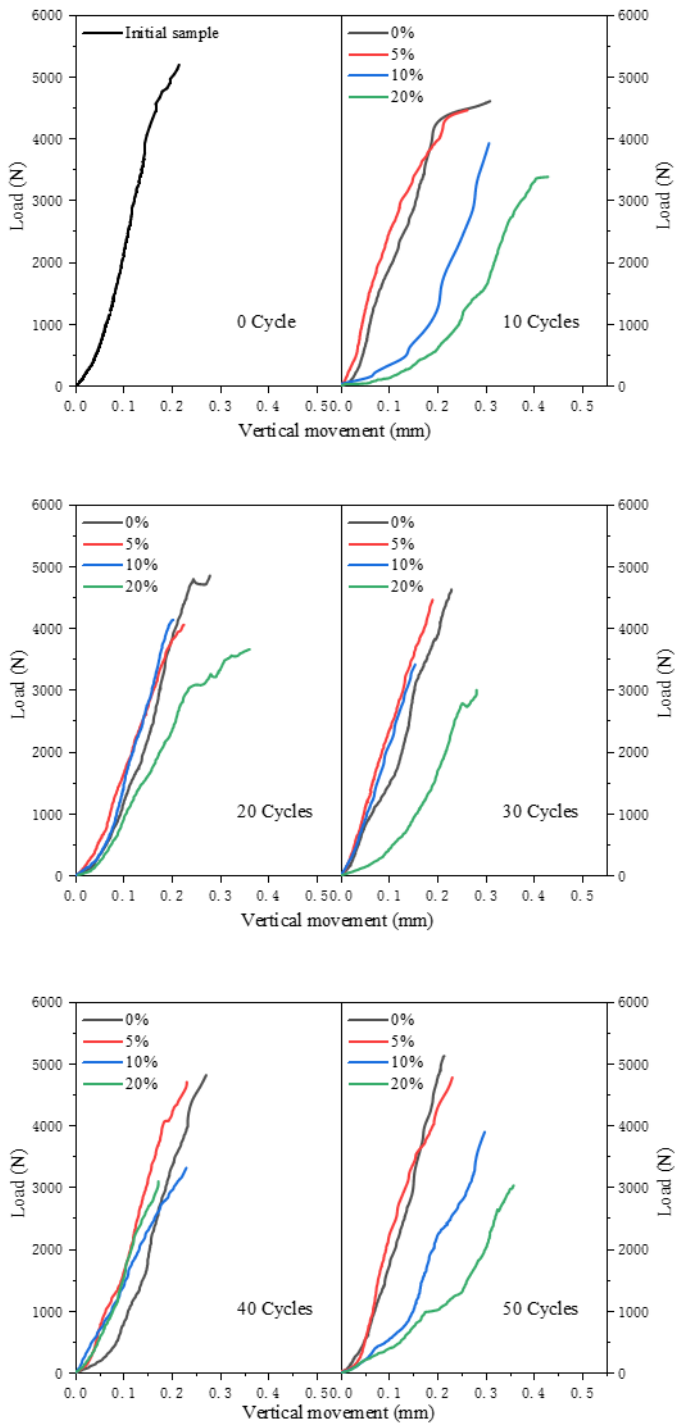


Figure 11

Point-load test load-movement deformation curve

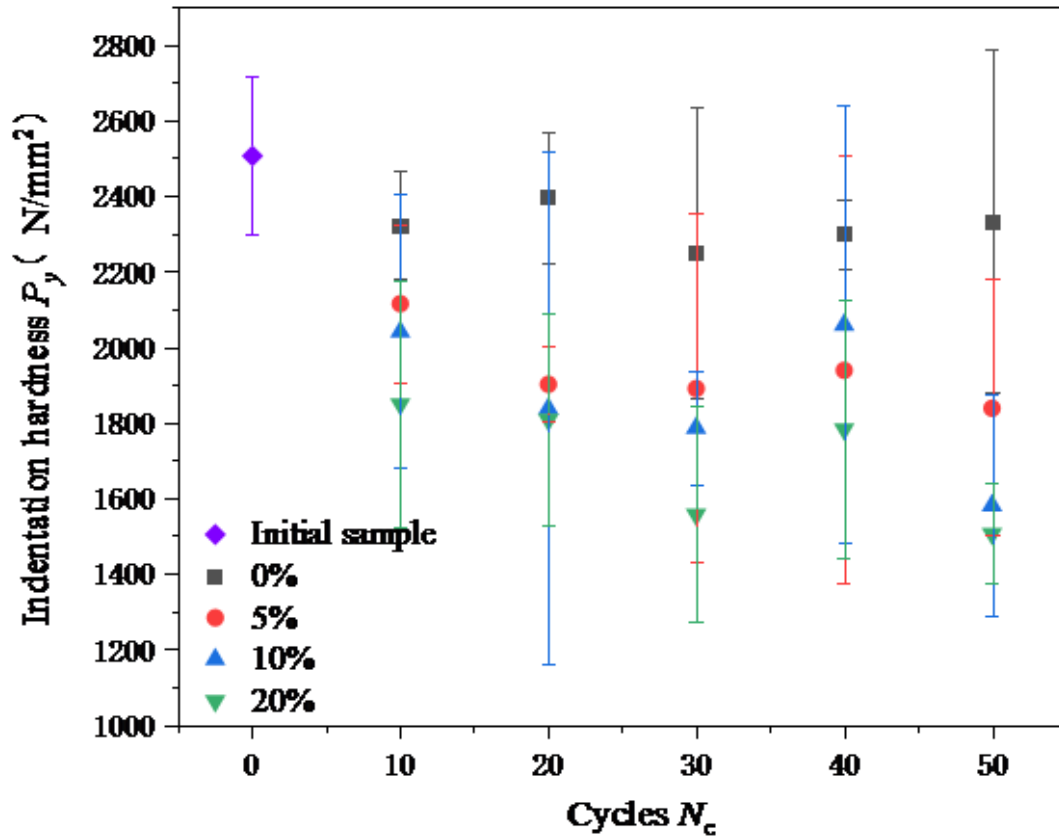


Figure 12

Variation in indentation hardness with cycle number from point-load tests

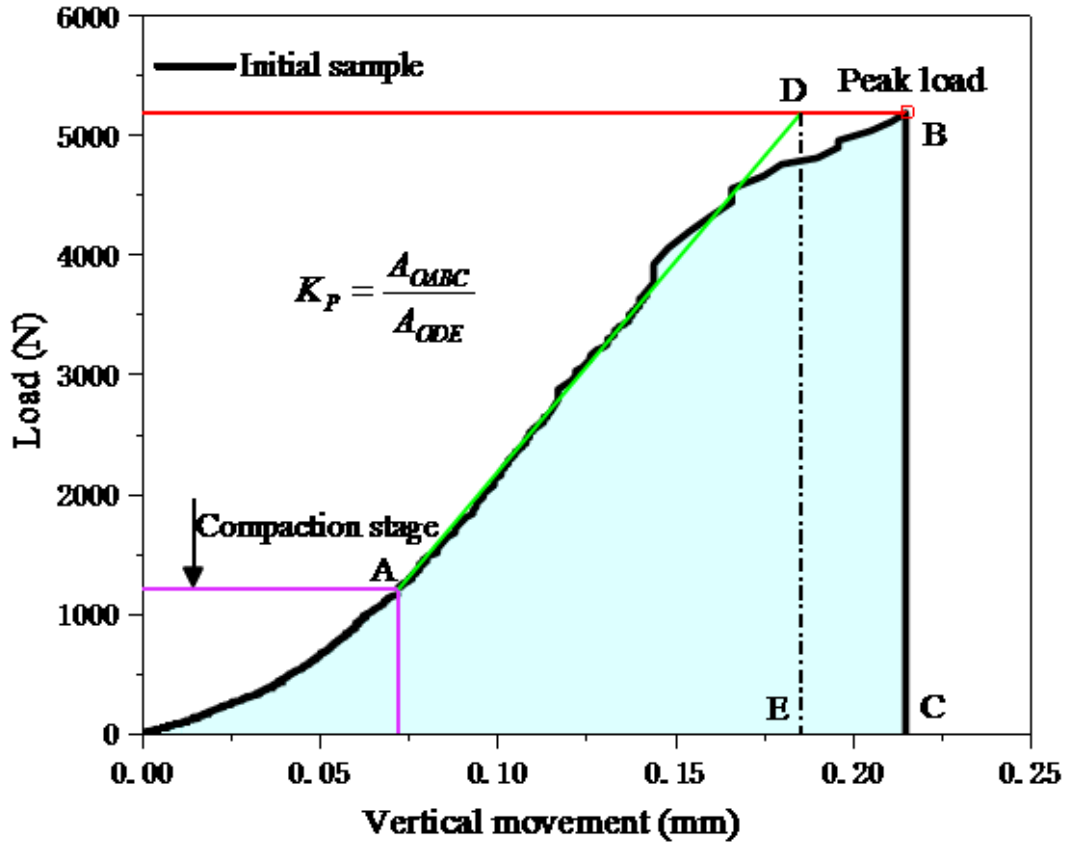


Figure 13

Plastic coefficient of the initial granite sample

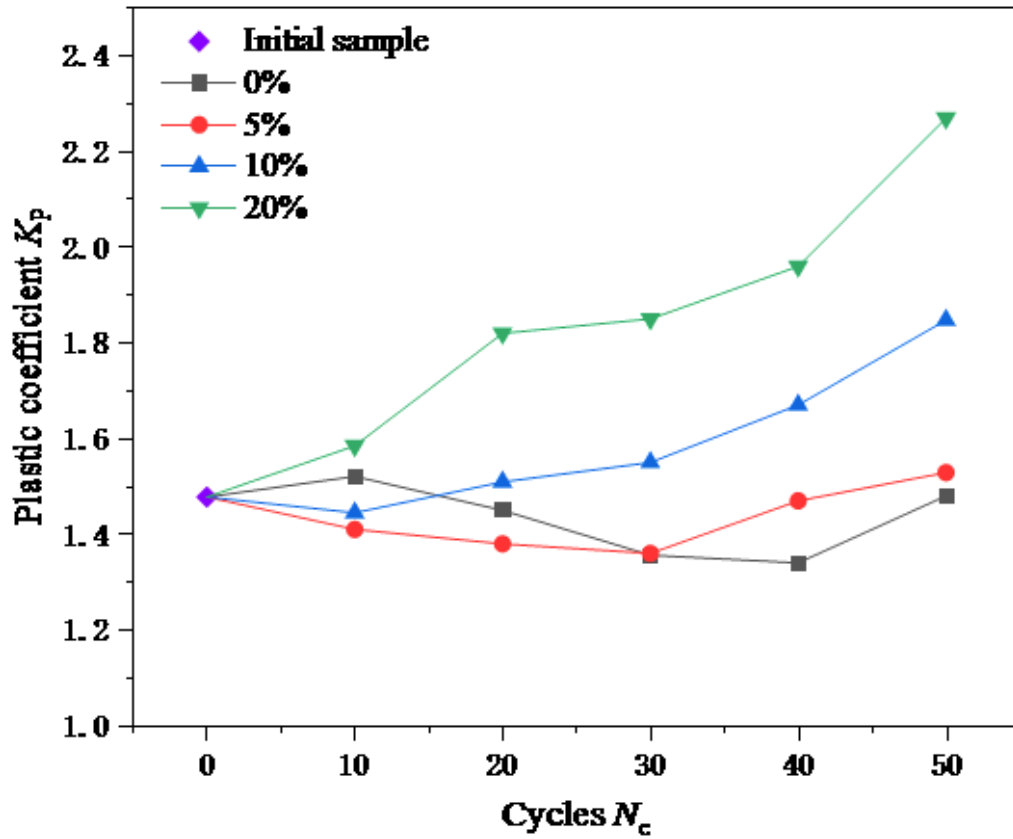


Figure 14

Variation in plasticity coefficient with cycle number

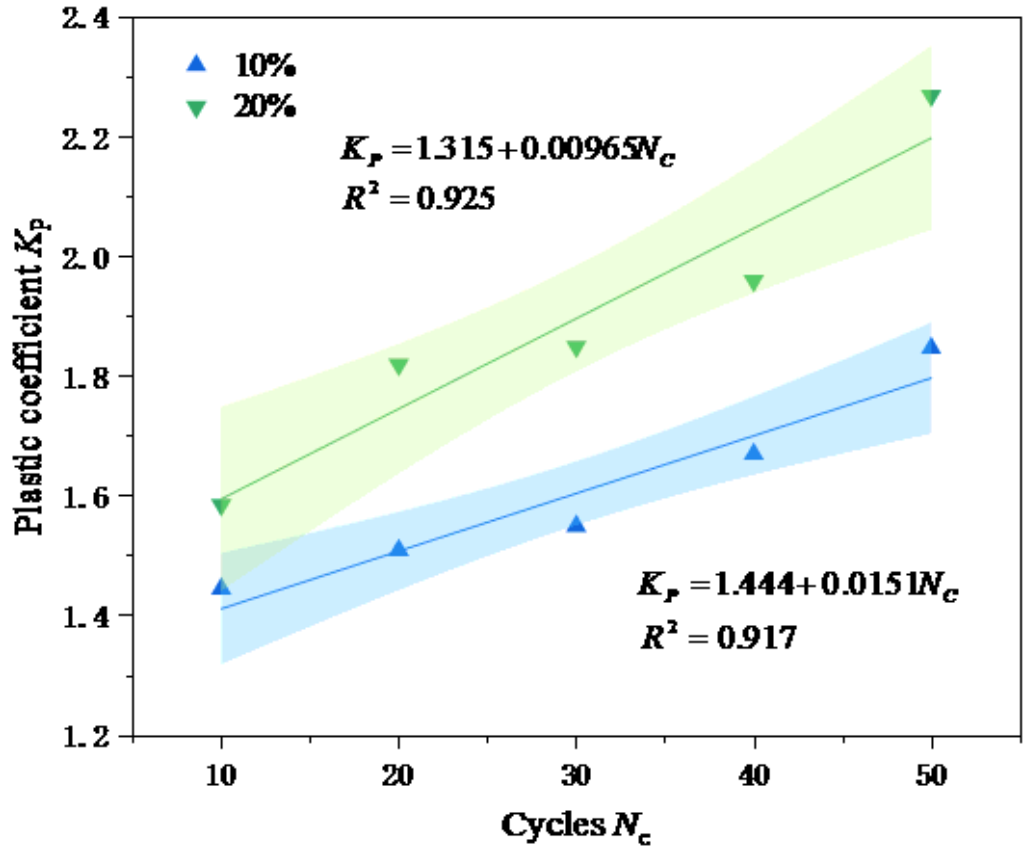


Figure 15

Changes in plasticity coefficient with cycle number for samples in 10% and 20% Na₂SO₄ solutions, with fitted curves

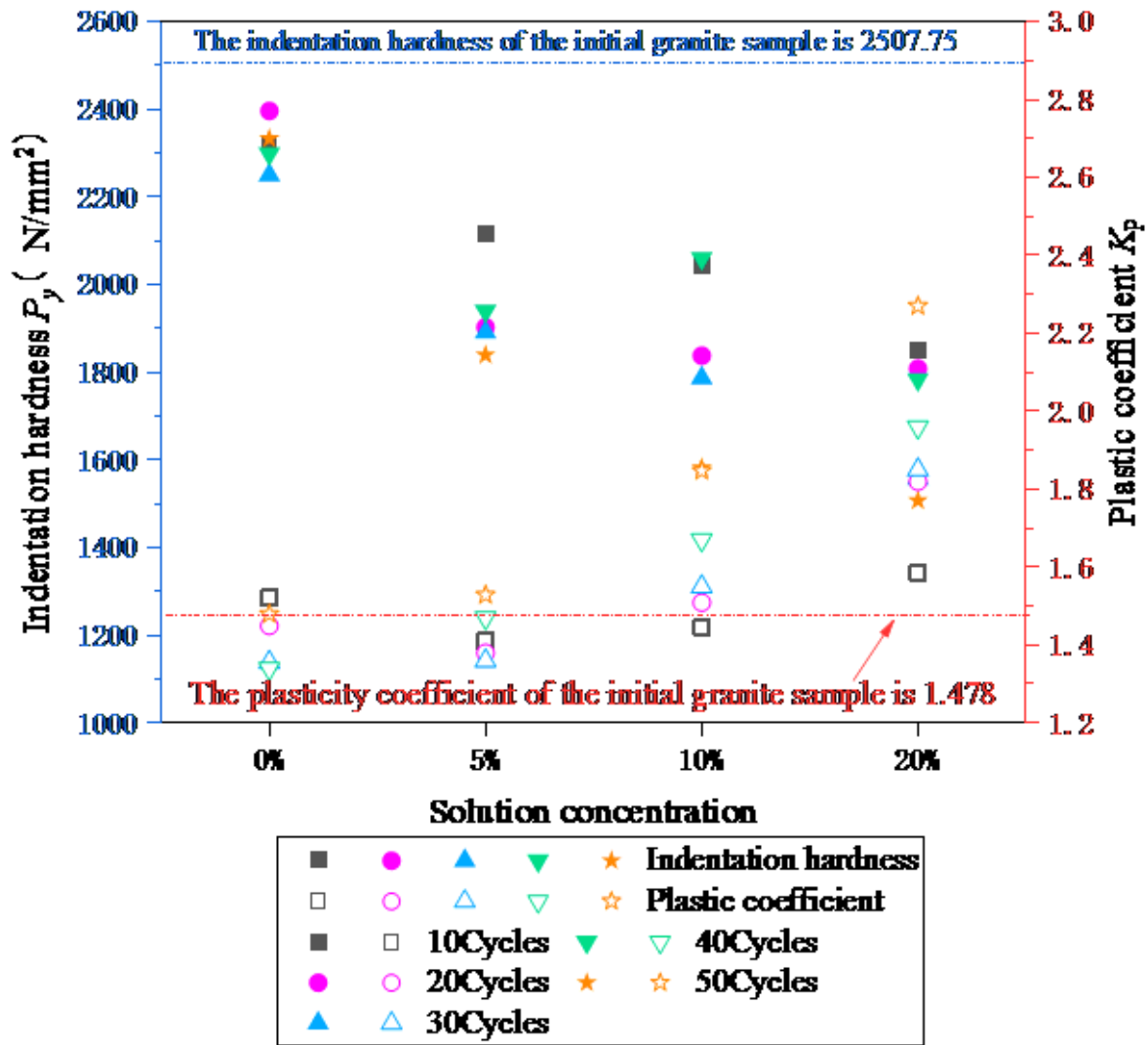


Figure 16

Relationship between hardness, plasticity coefficient and Na2SO4 solution concentration

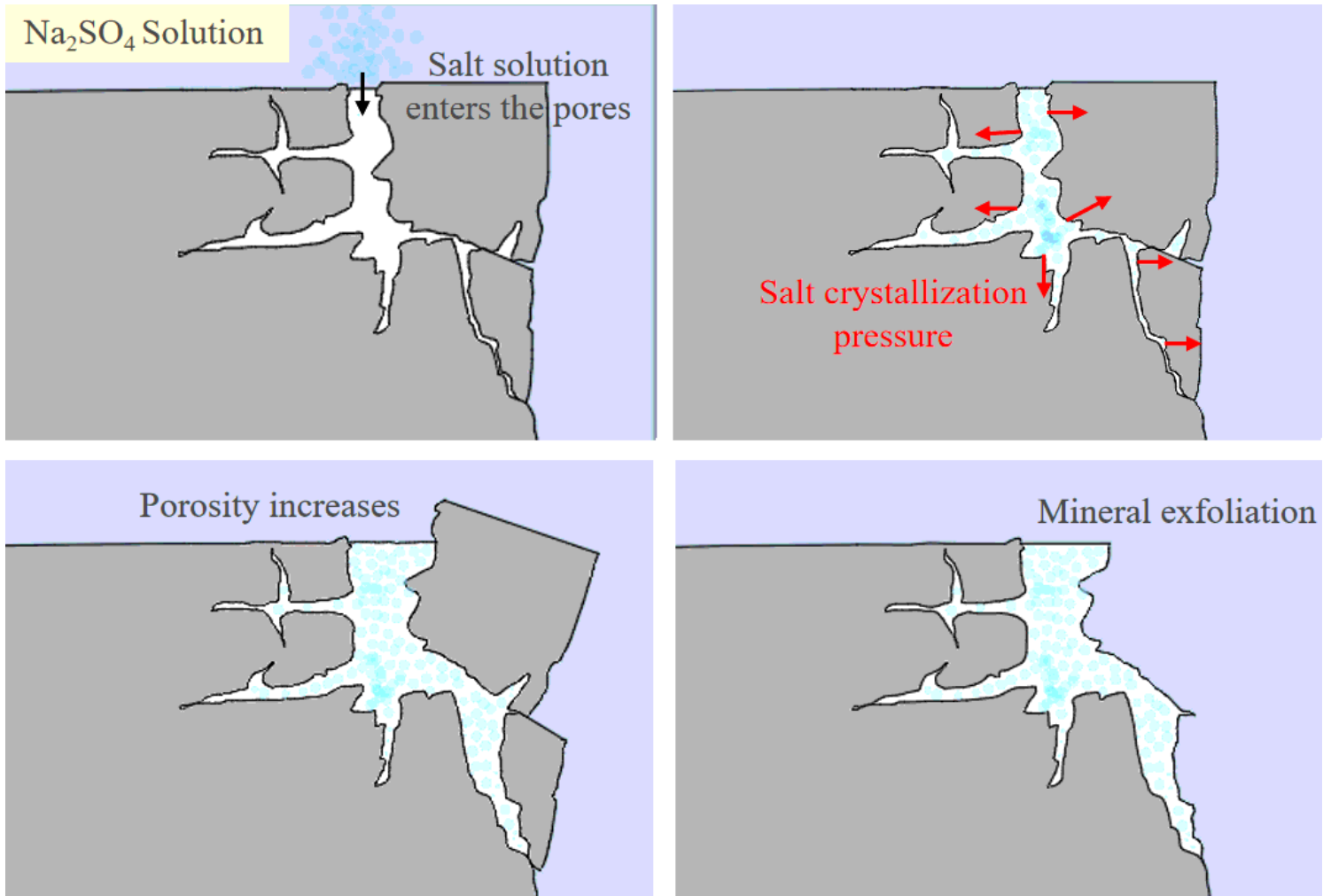


Figure 17

Rock failure diagram

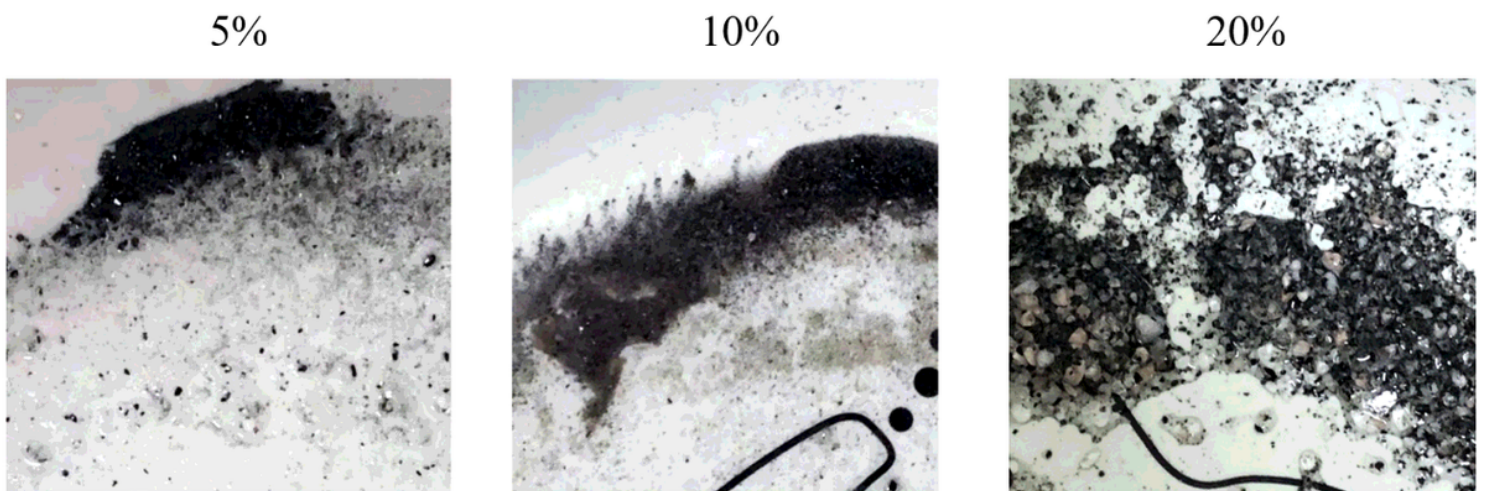


Figure 18

Shedding of minerals during wet-dry cycling